NJC

Accepted Manuscript

This is an *Accepted Manuscript*, which has been through the Royal Society of Chemistry peer review process and has been accepted for publication.

Accepted Manuscripts are published online shortly after acceptance, before technical editing, formatting and proof reading. Using this free service, authors can make their results available to the community, in citable form, before we publish the edited article. We will replace this *Accepted Manuscript* with the edited and formatted *Advance Article* as soon as it is available.

You can find more information about *Accepted Manuscripts* in the Information for Authors.

Please note that technical editing may introduce minor changes to the text and/or graphics, which may alter content. The journal's standard Terms & Conditions and the Ethical guidelines still apply. In no event shall the Royal Society of Chemistry be held responsible for any errors or omissions in this *Accepted Manuscript* or any consequences arising from the use of any information it contains.

ROYAL SOCIETY OF CHEMISTRY

www.rsc.org/njc

Nitrogen-Doped Mesoporous Carbon Hollow Spheres as Novel Carbon Support for Oxygen Reduction Reaction

Chun-Han Hsu[1], Jhan-Yi Jan[1], Hong-Ping Lin[2] and Ping-Lin Kuo[*1]

[1]Department of Chemical Engineering, National Cheng Kung University, Tainan, Taiwan 70101 ROC

[2]Department of Chemistry, National Cheng Kung University, Tainan, Taiwan 70101 ROC

[*]Author to whom all correspondence should be addressed

Tel.: +886-6-275 7575; Fax: +886-6-276 2331

e-mail: plkuo@mail.ncku.edu.tw

Abstract

Novel nitrogen-doped mesoporous carbon hollow spheres (NMCs) as catalyst support are prepared using polyaniline as both carbon and nitrogen sources, where the amount of doped nitrogen is controllable (N/C ratio 7.81-16.83 wt%). The prepared NMCs are characterized via scanning electron microscopy, transmission electron microscopy, conductivity and nitrogen adsorption and desorption isotherms. For fuel cell application, a uniform dispersion of Pt nanoparticles with a diameter of 3.8±1.3 nm is anchored on the surface of the NMCs by ethylene glycol reduction. In a single cell test, the Pt/NMC catalyst is found to have superior catalytic activity to better support the oxygen reduction reaction, resulting in an enhancement of about 19 % in mass activity compared with that of the commercial Pt/C catalyst, E-TEK.

1. Introduction

Proton exchange membrane fuel cells (PEMFCs) have been of great interest as future energy sources for various applications, and have attracted much research work in this field [1-7]. However, the commercial possibility of the fuel cells has been hindered by several challenges, including poor kinetics of the oxygen reduction reaction (ORR), the high cost of noble metal catalysts and the loss of the electrochemically active surface area (EAS) of platinum. Studies have shown that Nitrogen-doped carbon materials (NCs) have been receiving considerable attention due to their unique properties such as conductivity, nanostructure and catalyst activity [8-13]. Several methods for preparing NCs have been used, such as direct doping during the synthesis of carbon materials and post-treatment of carbon materials with an N-containing precursor (N_2, NH_3, etc.). Additionally, Pt loaded onto NCs provides enhanced catalytic activity toward ORR [14-23].

Recently, in our laboratory, a high nitrogen-containing carbon layer on carbon nanotubes (NC-CNTs) was prepared with aniline, which acts bi-functionally: (1) to disperse the bundled CNTs into separated lines; and, (2) to be polymerized into polyaniline (PANI) and then carbonized to form the nitrogen-containing carbon layer surrounding the CNTs to act as carbon support [24-27]. Our preliminary findings indicate that the NC-CNTs function better as carbon supports than CNTs or commercial carbon spheres in fuel cells. Here, we prepared novel nitrogen-doped mesoporous carbon hollow spheres (NMCs) by carbonization of polyaniline on mesoporous silica hollow sphere templates. The N/C ratio can be easily controlled by

controlling the amount of polyaniline and carbonization temperature. Moreover, the hollow-structured nitrogen-doped mesoporous carbon with high surface area can be obtained via hard template method compared to the previously reported [28-30]. Then, this was followed by the synthesis of small and homogeneous Pt particles on the NMCs to obtain Pt/NMC. Enhancements in the conductivity and oxygen reduction activity, attributed to the unique structure of the NMCs, were found as compared with the properties of Pt loaded on NMCs or the commercial catalyst E-TEK (Pt/XC-72). Furthermore, systematic experiments were conducted to investigate the nitrogen-containing effects on NMC.

2. Experimental

2.1 Synthesis of NMCs

Mesoporous carbon hollow spheres (MC) and mesoporous silica hollow spheres (MS) were synthesized using a method reported in the literature [31, 32]. Polyethylene oxide/phenol formaldehyde silica composite (PEO-PF/silica) hollow spheres were obtained from a fast silicification of a polymer blend, which contained polyethylene oxide (PEO) as silica gelator and phenol formaldehyde (PF) polymer as carbon source, in a highly diluted silica solution at pH of approximately to 5.0-6.0. The PF-PEO/silica hollow spheres can be easily converted to MS by hydrothermal treatment and calcination, and to MC after pyrolysis under a nitrogen atmosphere and silica etching. The NMC nanocomposites were synthesized by chemical oxidation polymerization of aniline on an MS template. 1.50 g of aniline monomers in 60 mL 0.5 M H_2SO_4 containing 0.50 g MS was first stirred before the synthesis. Then, a 0.50 M H_2SO_4

solution containing 2.30 g of the oxidant $(NH_4)_2S_2O_8$ (ammonium peroxodisulphate, APS) was added. The subsequent polymerization was carried out at room temperature for 24 h. The resulting products were filtered and washed with deionized water, and then dried under vacuum at 70 ^oC overnight. The PANI/MS hybrid materials were treated at various temperatures (from 550 to 850 ^oC) in an argon gas flow oven (150 sccm) for 4 h to form a NMC/MS. After removing the MS template by 3.0 M $NaOH_{(aq)}$, the final products so-fabricated were denoted as NMC-*x*, where *x* is the carbonization temperature (^oC).

2.2 Loading of Pt colloids on carbon supports

The Pt catalysts were prepared by the ethylene glycol (EG) reduction method [33-35]. The 20 wt% Pt/C catalysts were prepared by combining the Pt solutions with a suspension of NMC support in solution. 60.0 mg of NMC, 20 wt% Pt solution, and 100 mL EG were then added into a glass flask. The solution was refluxed at 160 ^oC with magnetic stirring for 2 hr. The resulting solids were washed with copious amounts of distilled water, and dried at 70 ^oC.

2.3 Sample characterization

The morphological characterization was performed by field emission scanning electron microscope (FE-SEM) using a JEOL JEM6700 FESEM operating at 10 kV while transmission electron microscopy (TEM) was conducted using a Hitachi H-7500 microscope operating at 80 kV. Specific surface areas of the prepared samples were determined using the Brunauer-Emmett-Teller (BET) method on a Micromeritics ASAP 2020 instrument. Electrical conductivity in a pressed pellet mixed with 5wt% polytetrafluoroethylene was measured by

four-point probe under a pressure of 20 MPa at room temperature. Further, TG analysis was performed on a thermogravimetric analyzer (TGA Q-500) over a temperature range of 50-800 ^{o}C under an air atmosphere at a heating rate of 20 ^{o}C min^{-1}. And finally, the structures of the samples were characterized by a X-ray diffraction (XRD) using RIGAKU D/MAX with a step size of 0.01^{o} and Cu-Kα radiation (λ：1.5405Å) operated at 30 kV and 30 mA.

2.4 Electrochemical measurements

A CHI-608A potentiostat/galvanostat and a conventional three-electrode test cell were used for electrochemical measurements while a GC disk electrode (5 mm diameter, Pine) served as the substrate for the supported catalyst. An catalyst suspension aliquot (2mg catalyst dispersed in 2ml IPA) was transferred onto the carbon substrate, leading to a catalyst loading of 50.9 μg catalyst cm^{-2} for Pt/NMC, Pt/MC and E-TEK. Cyclic voltammetry (CV) with a scan rate of 10 10 mV s^{-1} was performed on the working electrode by cycling the voltage between 0 and 0.8 V versus Ag/AgCl reference electrode in O_2-saturated 0.1 M $HClO_4$ solution.

A single fuel cell test was evaluated using a unit cell with an active area of 5 cm^2 fed with a methanol flow rate of 2.0 mL min^{-1} at the anode, and an oxygen rate of 200 sccm at the cathode. The membrane electrode assemblies (MEA) for the single cell test were fabricated as follows. Catalyst ink was prepared by mixing Pt/C catalyst powder with water (2.0 mL per 1.0 g of electrocatalyst), followed by the addition of isopropanol (20.0 mL per 1.0 g of electrocatalyst) to prevent ignition. 5% Nafion dispersion (Dupont) was added (0.80 g solid Nafion per 1.0 g of catalyst) to the catalyst slurry. Catalyst coating on gas diffusion layers (GDLs) (50 wt%

wet-proofing carbon paper, Toray) with a 5.0 cm^2 active area was prepared by brushing Pt/C catalyst ink. The catalyst loadings on the anode and cathode layers were both 1.0 mg Pt cm^{-2}. The catalyst-coated GDLs were hot-pressed with a Nafion-117 membrane (Du Pont) at 140 ^oC under 30.0 kg cm^{-2} of pressure. All MEAs were tested at 70 ^oC.

3. Results and discussion

3.1 Structure properties of NMC at different pyrolysis temperatures

The MS and MC were synthesized by a templating method, starting with phenol formaldehyde polymer as the carbon precursor and using PEO polymer as a structure-directing agent. [31, 32] The PF-PEO/silica hollow spheres can be feasibly converted to MS by hydrothermal treatment and calcination, and subsequently to MC after pyrolysis under a nitrogen atmosphere and silica etching. The NMC nanocomposites were synthesized by the chemical oxidation polymerization of aniline on an MS template to obtain the PANI/MS hybrid materials. Then, the NMC samples were prepared by carbonization and removed of the MS template. Morphologies of the MS, MC, and NMC samples were characterized by SEM, as shown in Figures 1a-c, respectively. Figures 1a and 1b respectively show that MS and MC were uniform and spherical with a diameter of approximately 500 nm. Examination of the broken spheres confirmed that they have spherical hollow cores with a shell thickness ranging from 50 to 70 nm. Under the influence of the polyaniline coating and carbonization, the synthesized NMCs (see Figure 1c) were uniform and spherical with a diameter of roughly 500 nm. TEM was

used to further investigate the state of the MS, MC, and NMC samples, the results of which are shown in Figures 1d-f, respectively. The obtained grain sizes of the samples are in agreement with their apparent sizes determined by SEM.

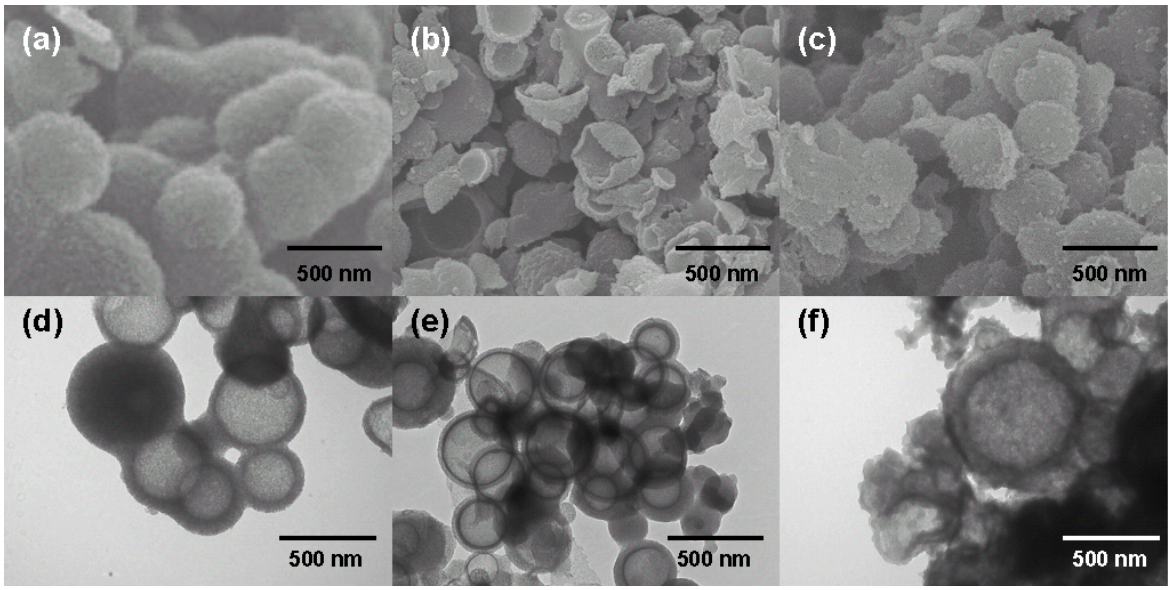

Figure 1. SEM images of (a) mesoporous silica hollow sphere (MS), (b) mesoporous carbon hollow sphere (MC) and (c) nitrogen-doped mesoporous carbon hollow sphere (NMC). TEM images of (d) MS, (e) MC and (f) NMC.

NMCs were prepared using polyaniline as a carbon and nitrogen source coated on the surface of MS. The so-obtained NMCs were named NMC-*x*, where *x* is the carbonization temperature (^{o}C). The surface areas of pristine MC and NMC-*x* were measured by N_2 adsorption/desorption isotherms measurements performed at 77 K (Table 1). The NMC-850 sample had a larger surface area (994 m^2 g^{-1}) than both the NMC-700 (709 m^2 g^{-1}) and NMC-500 (671 m^2 g^{-1}) samples. It is known that a higher surface area of carbon support will increase the depositing sites for accommodating more Pt nanoparticles. The structure parameters of MC and various NMC-*x* samples derived from N_2 adsorption/desorption data are summarized in Table 1.

The electrical conductivities of MC and NMC-*x* were further characterized by the four-point probe method, also shown in Table 1. Pristine MC exhibited an electrical conductivity of 0.0039 S cm^{-1}, while NMC-850 and NMC-700 showed higher electrical conductivities, i.e. 3.6 and 0.027 S cm^{-1}, respectively. Evidently, the amorphous carbon char formed at lower carbonization temperatures resulted in a decrease in electrical conductivity, for example, NMC550 has a low electrical conductivity value of $2*10^{-6}$ S cm^{-1}; however, the electrical conductivity of NMC-850 is comparable to that of the commercial carbon support XC-72 (6.2 S cm^{-1}). The observations of NMC-550 to NMC-850 with an N/C ratio from 16.8 % to 7.8 %, as determined by EDS analysis, strongly suggests that the N/C ratio can be easily controlled by changing the carbonization temperature, the results of which are also shown in Table 1.

Table 1. Physicochemical properties of NMC-850, NMC-700, NMC-550 and MC samples.

	N/C[a] (%)	**S_{BET}[b] (m^2 g^{-1})**	**S_{micro}[c] (m^2 g^{-1})**	**V_{total} (cm^3 g^{-1})**	**Conductivity[d] (S cm^{-1})**
NMC-850	7.81	994	472	1.39	3.6
NMC-700	12.58	709	395	0.84	0.027
NMC-550	16.83	671	276	0.88	$2*10^{-6}$
MC	0	526	256	0.39	0.0039

[a]: Elemental composition measured by EDS;
[b]: S_{BET}: BET surface area;
[c]: S_{micro}: micropore surface area;
[d]: Conductivity measured by four-point probe method.

In the XRD diagrams as shown in Figure 2a, the diffraction peaks at 2θ of 26.2° and 54.3° assigned to be the reflections from the (002) and (004) planes of carbon materials, respectively,

shows good crystallinity of the NMC. It is clear that the peak intensity of MC at 26.2° was low, bandwidths were broader, and the peak at 54.3° from (004) planes disappeared. This demonstrates the highly disorder structure of MC. Furthermore, the Raman spectroscopy of NMC, MC and XC-72 were shown in figure 2b, the analysis of the peak positions and intensities give the information about the carbon structure. Carbon materials exhibit two main characteristic absorptions: G-(~1580 cm^{-1}) and D-band (~1350 cm^{-1}). The ratio between the D band and G bands (I_D/I_G) is an indicator of the degree of disorder within the samples. The I_D/I_G ratios are 1.04, 1.02, and 1.09 for NMC-850, MC, and XC-72 samples, respectively. The low I_D/I_G ratio of NMC may due to the nitrogen-doped in the carbon structure.

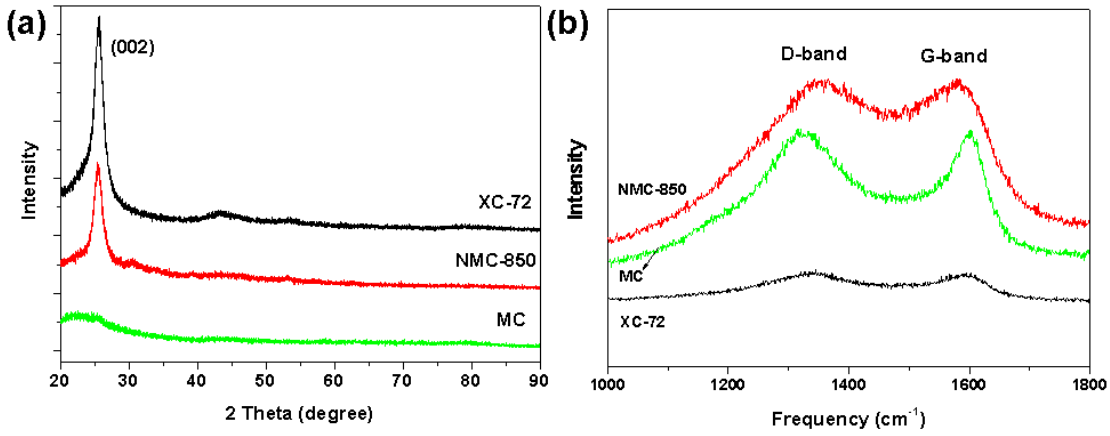

Figure 2. (a) XRD diagrams of NMC-850, MC and XC-72 (b) Raman curves of NMC-850, MC and XC-72

3.2 Properties and electrocatalytic performances of Pt/NMC

Here, NMC-850 was applied as carbon support for Pt loading, and its physical and electrochemical properties were investigated and compared with that of the XC-72 supported EG-reduced Pt (EG-Pt XC-72) catalyst. TEM images of the Pt nanoparticles on NMC, MC, and

EG-Pt/XC-72 are shown in Figures 3a-c. The prepared Pt nanoparticles were well-dispersed on NMC with diameters in the range of 3.8±1.3 nm, as summarized in Table 2. For comparison, the Pt supported on MC (Figure 3b) and XC-72 (Figure 3c) was prepared under the same conditions, of which the diameters measured about 5.6±1.7 and 3.5±0.7 nm, respectively. The corresponding histogram reveals that the size distribution was relatively narrow and nearly monodispersed for Pt/NMC. This clearly indicates that ethylene glycol effectively stabilizes Pt nanoparticles, both on MC and XC-72, but more obviously so on NMC. This, in turn, means that the presence of these homogeneously distributed nitrogen species on the surfaces of the NMC shells effectively provides stabilizer sites for the reduction of Pt^{4+} by ethylene glycol, which favors forming small Pt particles. Total Pt loading (wt%) was quantified by thermogravimetric analysis (TGA), also as shown in Table 2.

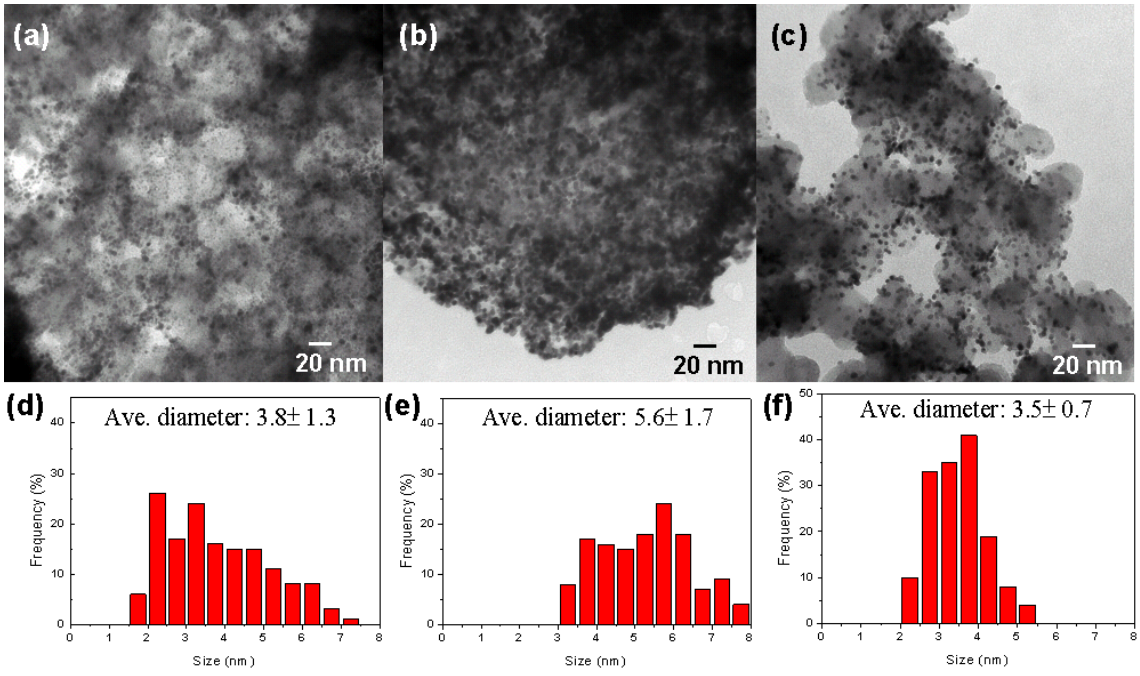

Figure 3. TEM images of (a) Pt/NMC, (b) Pt/MC and (c) EG-Pt/XC-72 catalyst and their size distribution diagrams (d-f, respectively).

Table 2. Physicochemical properties and electrochemical performance of Pt nanoparticles supported on NMC, MC and XC-72 carbon materials.

Electrode	Pt loading (wt%)	Particle size[a] (nm)	$E_{1/2}$ (V)[b]	Mass activity[c] (A gPt^{-1})	Power density[d] (mW cm^{-2})
Pt/NMC	19	3.8±1.3	0.46	23.1	25.2
Pt/MC	20	5.6±1.7	0.39	11.1	9.2
EG-Pt/XC-72	20	3.5±0.7	0.38	8.6	14.6

[a] Particles size from TEM

[b] v.s. Ag/AgCl

[c] mass activity data was calculated from CV curve

[d] power density data was calculated from the single cell test

The powder XRD patterns of the Pt nanoparticle supported on different carbon materials are shown in Figure 4. The diffraction peaks in the XRD pattern at 2θ of 39.6°, 46.1°, 67.5°, and 81.2° can be assigned as the reflections from the (111), (200), (220), and (311) planes of the face-centered-cubic (fcc) Pt, respectively, indicating the existence of good crystallinity. The bandwidths become slightly sharper for the Pt/MC catalyst, indicating an increase in particle size.

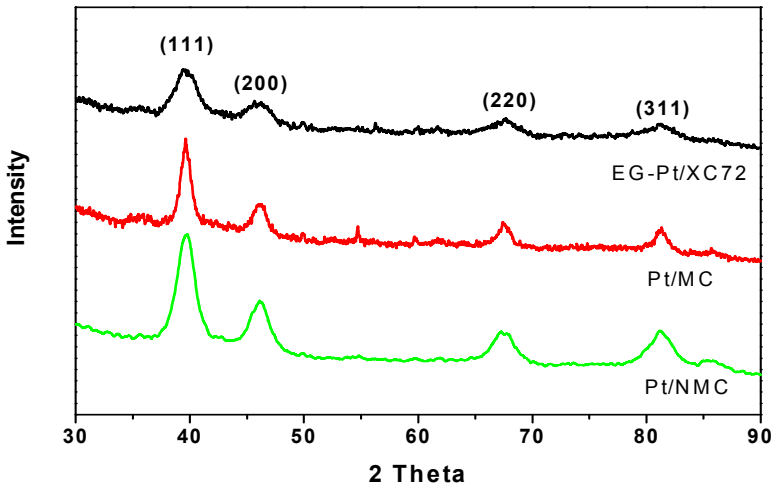

Figure 4. XRD diagram of Pt/NMC, Pt/MC and EG-Pt/XC-72 catalysts.

The catalytic activity of the Pt/NMC catalyst (Figure 5a) for the oxygen reduction reaction was studied using CV and RDE voltammetry. For comparison, ORR measurements were performed on 10 µg of Pt/NMC, Pt/MC, and EG-Pt/XC-72 catalysts in O_2 saturated 0.10 M $HClO_{4(aq)}$ electrolyte. The scan rate was 10 mV s^{-1} with a rotation rate of 2500 rpm. The ORR half-wave potentials for the Pt/NMC (0.45 V) were higher than that of the Pt/MC (0.37 V) and EG-Pt/XC-72 (0.38 V) catalysts, indicating that Pt/NMC has higher catalytic activity than the others. Furthermore, the CV curve for carbon material (Figure 5b) showed a significant positive shift in the reduction peak while a high steady-state diffusion current was observed for NMC compared to MC and XC-72. This implies that NMC is more catalytically active for ORR.

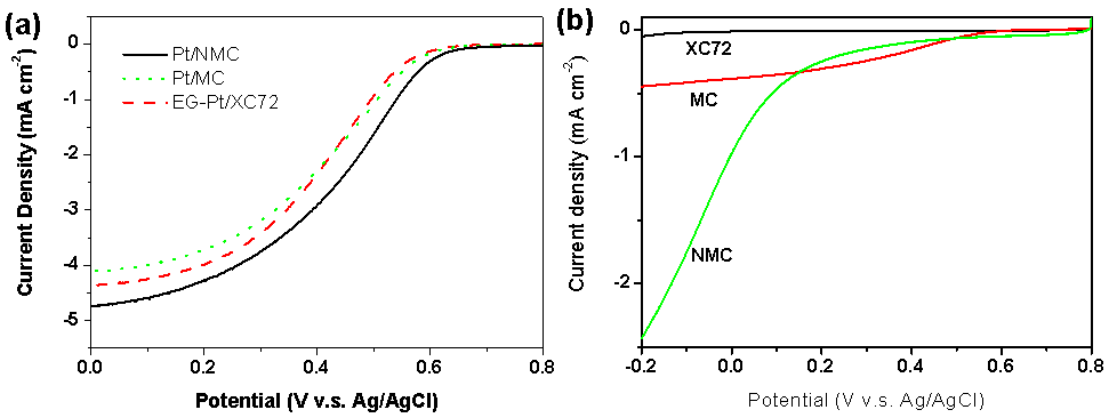

Figure 5. CV curves of (a) Pt/NMC, Pt/MC and EG-Pt/XC-72 catalyst, and (b) NMC, MC and XC-72 carbon material at a scan rate of 10 mV s^{-1}.

To probe the benefits of this novel carbon support, the Pt/NMC, Pt/MC, EG-Pt/XC-72 and commercial 20wt% Pt/XC-72 catalysts (E-TEK) were used as anodes. In each fuel cell test, E-TEK was used as cathode, Pt loading was 1.0 mg cm^{-2}, and the power density curves **(Figure 6)** of the single DMFC at 70 ^{o}C were evaluated. Compared with E-TEK, an improved

polarization behavior was observed from the NMC-based electrode. Moreover, the mass activity of Pt for the Pt/NMC-800 sample was 25.2 mW mg^{-1} Pt, which is about 19%, 69% and 180% higher than that of E-TEK (21.2 mW mg^{-1} Pt), EG-Pt/XC-72 (14.9 mW mg^{-1} Pt), and Pt/MC (9.1 mW mg^{-1} Pt), respectively. The superior electrocatalytic activity of Pt/NMCs is tentatively attributed to the following higher oxygen reduction activity on the NMCs. Therefore, the presence of these homogeneously distributed nitrogen species on the surfaces of the NMC shells apparently plays an important role for Pt loading.

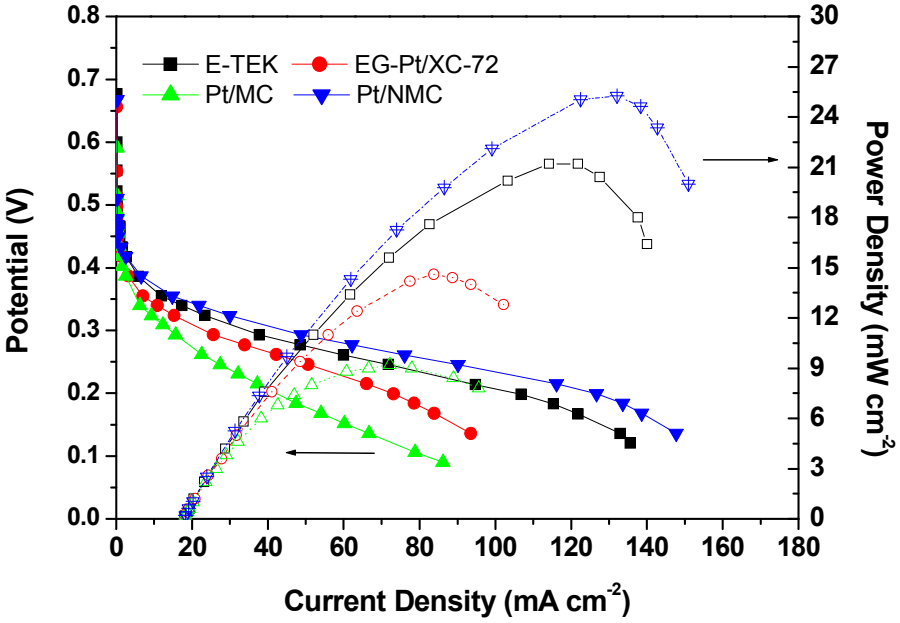

Figure 6. Performance of Pt/NMC, Pt/MC, EG-Pt/XC-72 and E-TEK catalysts as DMFC anode at 70 ^{o}C. Fuel feed: 2.0 M CH_3OH 2.0 mL min^{-1}; oxygen feed: 100 sccm.

4. Conclusions

Novel nitrogen-doped mesoporous carbon as carbon support was been successfully prepared

using polyaniline as a source of carbon and nitrogen, where the amount of doped nitrogen is controllable form N/C ratio 7.81 to 16.83 wt%. The SEM results show that the nitrogen-doped mesoporous carbon have hollow sphere morphology. A small and uniform dispersion of Pt nanoparticles with a diameter of 3.8±1.3 nm was then anchored on the surface of the nitrogen-doped mesoporous carbon hollow spheres, for which the Pt nanoparticles were prepared using ethylene glycol. The cyclic voltammetry measurements showed that the nitrogen-doped mesoporous carbon have higher oxygen reduction activity than either mesoporours carbon or Vulcan XC-72. Furthermore, the nitrogen mesoporous carbon supported Pt catalyst has enhanced catalytic activity toward oxygen reduction reaction and considerably improved performance, resulting in an enhancement of about 19% in mass activity compared with that of commercial 20wt% Pt/XC-72 catalyst, E-TEK. The successful advancement in this nitrogen-doped nanostructured carbon for fuel cell catalyst presents a significant achievement in both the scientific and engineering fields.

Acknowledgment The authors would like to thank the Ministry of Science and Technology, Taipei, R. O. C. for their generous financial support of this research.

References

1. Xu, W.; Zhou, X.; Liu, C. ; Xing, W.; Lu, T. *Electrochem. Commun.* **2007**, *9*, 1002-1006.
2. Wang, X.; Lee, J. S.; Zhu, Q.; Liu, J.; Wang, Y.; Dai, S. *Chem. Mater.* **2010**, *22*, 2178-2180.

3. Li, W.; Wang, X.; Chen, Z.; Waje, M.; Yan, Y. *Langmuir* **2005**, *21*, 9386-9389.

4. P. L. Kuo, C. H. Hsu, W. T. Li, J. Y. Jhan, W. F. Chen, *J. Power Sources* **2010**, *195*, 7983-7990.

5. Jin, C.; Nagaiah, T. C.; Xia, W.; Spliethoff, B.; Wang, S.; Bron, M.; Schuhmann, W.; Muhler, M. *Nanoscale* **2010**, *2*, 981-987.

5. Prabhuram, J.; Zhao, T. S.; Tang, Z. K.; Chen, R.; Liang, Z. X. *J. Phys. Chem. B* **2006**, *110*, 5245-5252.

6. Wang, X.; Li, W.; Chen, Z.; Waje, M.; Yan, Y. *J. Power Sources* **2006**, *158*, 154-159.

8. Chen, W. F.; Wang, J. P.; Hsu, C. H.; Jhan, J. Y.; Teng, Hsisheng; Kuo, P. L. *J. Phys. Chem. C* **2010.** *114***,** 6976-6982.

9. Hsu, C. H.; Liao, H. Y.; Kuo, P. L. *J. Phys. Chem. C*, 7933, 114, **2010,** *114***,** 7933-7939.

10. S. Sun, F. Jaouen, J.-P. Dodelet, *Adv. Mater.* **2008**, *20*, 3900-3904.

11. Z. Chen, M. Waje, W. Li, Y. Yan, *Angew. Chem. Int. Ed.* **2007**, *46*, 4060-4063.

12. M. K. Debe, A. K. Schmoeckel, G. D. Vernstrom, R. Atanasoski, *J. Power Sources* **2006**, *161*, 1002-1011.

13. C. M. Chuang, S. P. Sharma, J. M. Ting, H. P. Lin, H. Teng, C. W. Huang, *Diam. Relat. Mater.* **2008**, *17*, 606-610.

14. Gong, K.; Du, F.; Xia, Z.; Durstock, M.; Dai, L. *Science* **2009**, *323*, 760-764.

15. Bezerra. C. W. B.; Zhang, L.; Lee, K.: Liu, H.; Marques, A. L. B. ; Marques, E. P. ; Wang, H. ; Zhang, *Electrochim. Acta* **2008**, *53*, 4937-4951.

16. Shao, Y.; Sui, J.; Yin, G.; Gao, Y. *Appl. Catal. B-Environ*. **2008**, *79*, 89-99.

17. Yang, J.; Liu, D. J.; Kariuki, N. N.; Chen, L. X. *Chem. Commun*. **2008**, 329-331.

18. Jiang, L. Q.; Gao, L. *Carbon* **2003**, *41* , 2923-2929.

19. Ewels, C. P.; Glerup, M. *J. Nanosci. Nanotechnol.* **2005**, *5*, 1345-1363.

20. Sidik, R. A.; Anderson, A. B.; Subramanian, N. P.; Kumaraguru, S. P.; Popov, B. N. *J. Phys. Chem. B* **2006**, *110*, 1787-1793.

21. Jaouen, F.; Lefevre, M.; Dodelet, J. P.; Cai, M. *J. Phys. Chem. B* **2006**, *110*, 5553-5558.

22. Liu, R. L.; Wu, D. Q.; Feng, X. L.; Mullen, K. *Angew. Chem., Int. Ed.* **2010**, *49*, 2565.

23. Yang, W.; Fellinger, T. P.; Antonietti, M. *J. Am. Chem. Soc.* **2011**, *133*, 206

24. Hsu, C. H.; Wu, H. M.; Kuo, P. L. *Chem. Commun.* **2010,** *46*, 7628-7630.

25. Kuo, P. L.; Hsu, C. H. *ACS Appl. Mater. Inter.* **2011**, *3*, 115-118.

26. Hsu, C. H.; Kuo, P. L. *J. Power Sources* **2012**, *198*, 83-89.

27. Kuo, P. L.; Hsu, C. H.; Wu, H. M.; Hsu, W. S.; Kuo, D. *Fuel Cells* **2012**, *4*, 649-655.

28. Zhou, Y. K.; Neyerlin, K. N.; Olson, T. S.; Pylypenku, S.; Bult, J.; Dinh, H. N.; Gennett, T.; Shao, Z. P.; O'Hayre, R. *Energy Environ. Sci*. **2010**, *3*, 1437-1446.

29. Su, F.; Tian, Z.; Poh, C. K.; Wang, Z.; Lim, S. H.; Liu, Z.; Lin, J. *Chem. Mater.* **2010**, *22*, 832–839.

30. Qu, L.; Liu, Y.; Baek, J. B. ; Sai, L. *ACS Nano* **2010**, 4, 1321-1326.

31. Chang-Chien, C. Y.; Hsu, C. H.; Lee, T. Y.; Liu, C. W.; Wu, S. H.; Lin, H. P.; Tang, C. Y.; Lin, C. Y. *Eur. J. Inorg. Chem.* **2007**, *24* 3798-3804.

32. Chuang, C. M.; Sharma, S. P.; Ting, J. M.; Lin, H. P.; Teng, H. S.; Huang, C. W. *Diam. Relat. Mat.* **2008**, *17*, 606-610.

33. Bock, C.; Paquet, C.; Couillard, M.; Botton, G. A.; MacDougall, B. R. *J. Am. Chem. Soc.* **2004**, 126, 8028-8037.

34. Chen, W.; Zhao, J.; Lee, J. Y.; Liu, Z. *Mater. Chem. And Phys.* **2005**, 91, 124-129.

35. Yan, S.; Sun, G.; Tian, J.; Jiang, L.; Qi, Jing.; Xin, Qin. *Electrochimica Acta* **2006**, 52, 1692-1696.

Nitrogen-Doped Mesoporous Carbon Hollow Spheres as Novel Carbon Support for Oxygen Reduction Reaction

Chun-Han Hsu, Jhan-Yi Jan, Hong-Ping Lin and Ping-Lin Kuo*

e-mail: plkuo@mail.ncku.edu.tw

Table of Contents (TOC)

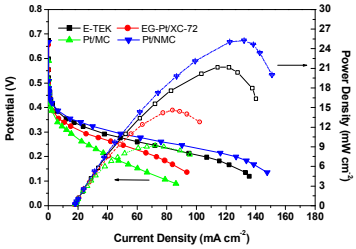

The Pt/NMC catalyst has better catalytic activity than that of Pt/MC, EG-Pt/XC-72 and the commercial Pt/C catalyst.